Passivity-Based Task Space Control of Hybrid Rigid-Soft (HyRiSo) Robots with Parametric Uncertainty

Lasitha Weerakoon[1] and Nikhil Chopra[1]

***Abstract*— This paper introduces a novel robotic system, coined as a hybrid rigid-soft (HyRiSo) robot composed of rigid links and soft links serially attached. HyRiSo combines the benefits of the dexterity of a soft manipulator with the support capability of a classical stiff arm. Due to the heterogeneous modes of actuation for the revolute joints and to enable the bending of the soft links, it is challenging to design an integrated controller for this class of robots. We demonstrate in this paper that the well-known passivity-based adaptive and robust controllers can be utilized to address this challenge. Specifically, we use these controllers for task space tracking in the presence of uncertain mass, stiffness, damping and actuation. We demonstrate the effectiveness of the proposed HyRiSo robot by showing task space tracking in the presence of complex obstacles and joint limits. We provide numerical examples using a 2-rigid-2-soft HyRiSo robot and compare the performance of the proposed task space controllers illustrating the efficacy of these frameworks.**

I. Introduction

Inspired by nature, the field of soft robotics has grown tremendously over the past few years due to the possibility of expanded manipulation capabilities over existing rigid robots in complex, unstructured environments [1], [2]. However, it is challenging to achieve precise motion control of complex multi-link soft robots in a large workspace. It has been observed that, increasing the length of the soft links induces workspace warping and makes the control problem harder [3]. While modern day rigid robots do not suffer from these challenges due to their precision, they lack the dexterity for completing task space operations, especially in cluttered environments [4]. On the other hand, the new class of robots discussed in this paper, the integrated hybrid rigid-soft (HyRiSo) robots, integrates the dexterity of a soft manipulator with the payload capacity and precision of a rigid robot.

An important observation for proposed class of hybrid robots is that heterogeneous actuation modalities are utilized for the revolute joints and the soft links. Thus, incorporating the uncertain actuator mapping from the pressure/current variables to the realized torques is important in the proposed control framework. Hence, developing a model-based integrated dynamic controller would be beneficial for fast autonomous operation as well as to understand the behavior of the HyRiSo robot and provide guarantees for stability and performance. Furthermore, as there could be uncertainties arising in the dynamic parameters of the robot, stiffness and damping terms of the soft links as well as lack of knowledge of the actuator mapping, it would be desirable to design controllers that are robust to such uncertainties.

In a previous related study, the authors in [5] proposed a control framework to control a rigid arm with an extruding soft manipulator used for berry picking. However, the rigid links and the soft link were separately controlled. While the performance was satisfactory, it was slow and required several user commands.

There have been several fundamental advancements to address the challenge of parametric uncertainty in classical rigid robotic control. Adaptive control laws for rigid robots have been proposed over the years [6], [7], [8], [9]. Robust controllers that are robust to uncertainty as well as the unmodeled disturbances have also been proposed [10], [11]. In [12], the authors introduced an adaptive controller for handling uncertainty in dynamic, kinematic as well as actuator parameters. In [13], the authors proposed an adaptive control framework to compensate for actuator failure in cooperative robots with uncertain parameters. Recently, the soft robotics community has also made progress toward handling the uncertainty in the control design. Among the few works, task space adaptive control for soft robots has been proposed in [14] and adaptive control has been used for bilateral teleoperation of soft robots in [15]. Curvature space adaptive control of soft robots using an augmented model has been proposed in [16], [17]. Several robust control approaches have also been proposed for soft robots [18].

However, an integrated control framework that addresses the model and actuation uncertainties in the class of HyRiSo robots is yet to be explored. To that end, in this paper we first propose the HyRiSo robot and then design passivity-based adaptive and robust controllers for task space trajectory tracking for this class of robots. Moreover, as the task space operation involve subtasks such as conforming to joint/curvature limits and collision avoidance with obstacles, we exploit the null space velocity to design subtasks to handle these issues and demonstrate the dexterity of the HyRiSo robot.

The main contributions of this paper is to propose the integrated HyRiSo robot for dexterous manipulation and to develop passivity based adaptive and robust controllers for this new system in the presence of parametric uncertainty in system dynamics as well in the actuator mapping. Additionally, we demonstrate the efficacy of HyRiSo robot for task space manipulation by exploiting the system redundancy to enable tracking in the presence of complex obstacles, joint limits, and unmodeled disturbances.

[1]Department of Mechanical Engineering, University of Maryland, College Park, MD 20742, USA. {lasitha,nchopra}@umd.edu

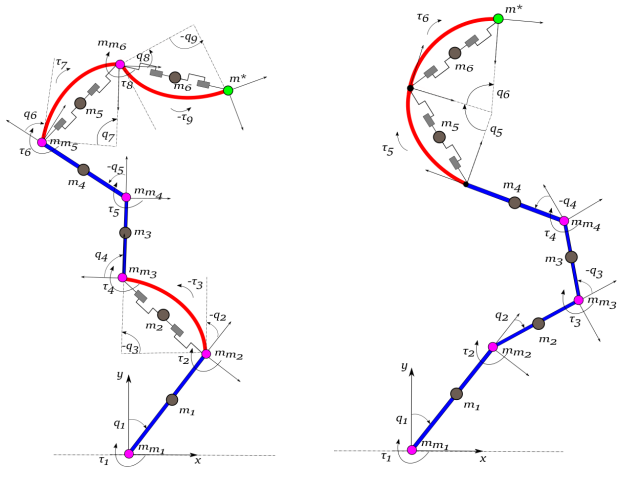

(a) RSRRSS HyRiSo robot (b) RRRRSS HyRiSo robot

Fig. 1. Two examples of HyRiSo robots composed of rigid (R) links (blue) and CC soft (S) links (red) modelled using the augmented formulation [20] are illustrated. The link masses m_i (brown), motor masses m_{m_i} (pink) and the end effector mass m^* (green) are also shown. The RSRRSS design (a) considers a HyRiSo robot with three R and three S links with all actuated revolute joints. The RRRRSS design (b) considers a HyRiSo robot with four R and two S links with fixed joints between R-S and S-S links.

II. The HyRiSo robotic system

A. Dynamics

Let us consider a robotic system with n_r rigid links (R) and n_s soft links (S) serially connected together forming an open chain of $n_s + n_r$ links. In the general setting, we will consider all the joints, R-R, R-S and S-S to be revolute joints. The soft links are assumed to be non-extensible and have a constant curvature (CC) [19]. In general, the hybrid robotic system will have $\alpha = n_r + 2n_s$ configuration variables for the system, namely the revolute joint angles (for all $n_r + n_s$ links), and the degree of curvature of the n_s soft links. We will denote them as q_i, with $i = 1, 2, ..., \alpha$ and collect them to the vector $q = [q_1, q_2, ..., q_\alpha]^\top \in \mathbb{R}^\alpha$. It should be noted that, in certain HyRiSo robot designs, we can also consider fixed joints between the R-S or S-S links. Two representative HyRiSo robots are shown in Fig.1.

We assume that the rigid links are uniform and the masses m_i, with $i \in \{\text{rigid link indices}\}$ are lumped at the centroid of the links. To accommodate motors at the revolute joints, we assume the motor masses m_{m_i}, with $i \in \{\text{revolute joint indices}\}$ to be lumped at the revolute joints. We also assume that the end effector mass m^* to be lumped at the robot's tip. Moreover, as the soft links are assumed to be CC, we will use the *augmented formulation* [20] to model the soft links. Using this formulation, the moment of inertia of the soft links are neglected since rotational kinetic energy is much smaller than the translational energy components [21]. The soft links masses m_i, with $i \in \{\text{soft link indices}\}$ are at the center of the main chord connecting the ends of the soft link. The dynamics of HyRiSo in the form is then written as,

$$M(q)\ddot{q} + C(q, \dot{q})\dot{q} + D\dot{q} + Kq + G(q) = \tau \qquad (1)$$

where $M(q) \in \mathbb{R}^{\alpha\times\alpha}$ is the inertia matrix, $C(q, \dot{q})\dot{q} \in \mathbb{R}^\alpha$ is the Coriolis and centrifugal terms, $G(q) \in \mathbb{R}^\alpha$ is the gravity vector and $\tau \in \mathbb{R}^\alpha$ is the control input vector. $D \in \mathbb{R}^{\alpha\times\alpha}$ and $K \in \mathbb{R}^{\alpha\times\alpha}$ are the damping and stiffness matrices respectively, which are assumed to be positive semi-definite diagonal matrices. Note that only the entries corresponding to the soft link will be non-zero in these damping and stiffness matrices. Here, as we are considering only the planar case, the task space of the robot is considered to be $\mathbb{R}^2$, and hence HyRiSo is a redundant robot. Moreover, as the dynamics of the HyRiSo robot is formulated in the Lagrangian form, we will utilize some useful properties such as the skew symmetric property and the linearly parameterizable property [22].

B. Actuator mapping via a transmission matrix

Assume a linear actuator mapping for the hybrid robot, $\tau = A\,p$, where $A \in \mathbb{R}^{\alpha\times\alpha}$ is the positive definite diagonal transmission matrix that maps the actuator signals $p \in \mathbb{R}^\alpha$ to the control torque τ. In HyRiSo robot, the actuator signals that need to be sent to the actuation units could be, for example, the current signals for motor torques or the pressure signals for pneumatic actuation for bending. While calibrating and obtaining the exact parameters for motor actuation can be done easily, obtaining these parameters for soft links is cumbersome. In the soft links, the torques applied by the soft links could be order of magnitude less than the torques applied by the motors. This poses challenges in practical implementations due to incorrect calibration. Moreover, the actuator parameters could change over time (albeit very slowly) due to several factors such as changes in the temperature [12]. Therefore, incorporating the actuator parameters and accounting for their uncertainty in the control design is of paramount importance. In several prior work that considered uncertainty in the actuator parameters, for example [12], the authors have used a separate parameter update law to update uncertain actuator parameters along with other parameter update laws for uncertain dynamics and kinematics.

In this work, we note a simple way to incorporate the actuator parameters as suggested in [23], [24]. Using the relationship of the actuator mapping for the torque on (1) and defining $M_0 = A^{-1}M$, $C_0 = A^{-1}C$, $D_0 = A^{-1}D$, $K_0 = A^{-1}K$ and $G_0 = A^{-1}G$ we can rewrite the dynamics,

$$M_0(q)\ddot{q} + C_0(q, \dot{q})\dot{q} + D_0\dot{q} + K_0 q + G_0(q) = p. \qquad (2)$$

We note that, since M, C and G are linear in the dynamic parameters so are M_0, C_0 and G_0 as premultiplication by A^{-1} is a linear operation. Therefore, M_0, C_0 and G_0 are linear in suitably selected parameters which are nonlinearly related with the dynamic parameters and the actuator mapping parameters. Therefore, we can extend the linear in parameters property of the dynamics to the system (2) such that for any differentiable vector $\gamma \in \mathbb{R}^\alpha$ there exists a regressor $Y_2(q, \dot{q}, \gamma, \dot{\gamma}) \in \mathbb{R}^{\alpha\times\beta_2}$ and a constant parameter vector $\Theta_2 \in \mathbb{R}^{\beta_2}$ such that $M_0(q)\dot{\gamma} + C_0(q, \dot{q})\gamma + D_0(q)\gamma + K_0 q + G_0(q) = Y_2(q, \dot{q}, \gamma, \dot{\gamma})\Theta_2$.

III. Passivity-Based Control for Hybrid Robots

In this section we design two passivity-based controllers, an adaptive controller and a robust controller, for task space trajectory tracking for HyRiSo robot. The proposed controllers are developed based on the Lagrangian formulation of the HyRiSo robots as given by (1), and follow similar ideas as provided in [7], [10]. However, the treatment for task space trajectory tracking closely relates to the methods implemented in bilateral teleoperation frameworks in [15], [25].

Consider the direct forward kinematics $h(\cdot) : \mathbb{R}^\alpha \to \mathbb{R}^2$ which maps the configuration space to the task space. Thus, the end effector position and the velocity are defined as, $X(t) = h(q)$ and $\dot{X}(t) = J(q)\dot{q}$, where, $J(q) = \frac{\partial h(q)}{\partial q} \in \mathbb{R}^{2\times\alpha}$ is the Jacobian matrix. Let $X_d(t)$ be the desired reference task space trajectory. Then, the tracking error is defined as $e(t) = X(t) - X_d(t)$. In order to drive the tracking error to approach origin, we will restrict it [25] to,

$$s(t) = \dot{q}(t) + J^+(q)\Lambda e(t) - \left(\mathbb{I}_\alpha - J^+(q)J(q)\right)\psi_s(t) \quad (3)$$

where, $\Lambda \in \mathbb{R}^{2\times2}$ is a positive definite gain matrix and $\mathbb{I}_\alpha$ is the $\alpha\times\alpha$ identity matrix. $\psi_s(t) \in \mathbb{R}^\alpha$ is the negative gradient of an appropriately defined convex function which is utilized for the subtask control (Sec IV). Here, $J^+ \triangleq J^\top(JJ^\top)^{-1} \in \mathbb{R}^{\alpha\times2}$ is the pseudo inverse of J and satisfies the property $JJ^+ = \mathbb{I}_2$. It is seen that once the trajectories reach $s = 0$,

$$\dot{e}(t) = -JJ^+\Lambda e(t) + J(\mathbb{I}_\alpha - J^+J)\psi_s = -\Lambda e(t) \quad (4)$$

and hence, the errors will reach the origin when $s = 0$.

Let us define signals, $v = \dot{q} - s$ and $a = \ddot{q} - \dot{s}$. Assuming uncertainty in the parameters, let us use the notation $\hat{(\cdot)}$ to denote the estimated values and $\tilde{(\cdot)}$ to denote the estimation error. Using the extended linear in parameters property of Lagrangian systems for the system (2), we can define the regressor $(Y_2\,(q, \dot{q}, v, a))$ and parameter (Θ_2) vector pair for the estimated systems,

$$\begin{aligned} Y_2(q, \dot{q}, v, a)\hat{\Theta}_2 =& \hat{M}_0(q)a + \hat{C}_0(q, \dot{q})v + \hat{D}_0 v \\ &+ \hat{K}_0 q + \hat{G}_0(q). \end{aligned} \quad (5)$$

Here we assume time invariant uncertainties in the dynamic terms, stiffness, damping and actuator parameters. Thus, the parameter vector Θ_2 is a constant.

A. Passivity-based adaptive control

Following the adaptive control approach [7], the control input for the HyRiSo robot is defined as,

$$p = Y_2(q, \dot{q}, v, a)\hat{\Theta}_2 - K_s s \quad (6)$$

where K_s is a positive definite diagonal gain matrix.

The dynamics of the closed loop system can be found by substituting the proposed control (6) in (2), and using (5),

$$M_0(q)\dot{s} + C_0(q, \dot{q})s + D_0 s + K_s s = Y_2(q, \dot{q}, v, a)\tilde{\Theta}_2 \quad (7)$$

where $\tilde{\Theta}_2 = \hat{\Theta}_2 - \Theta_2$. Let the adaptation law for the parameter estimation defined as,

$$\dot{\hat{\Theta}}_2 = -\Gamma Y_2^\top s \quad (8)$$

where Γ is a positive definite symmetric gain matrix that needs to be tuned.

Theorem 1: Consider the closed loop system (7) with the parameter adaptation law (8) and sliding surface (3). In the absence of any external wrenches, the task space position error (e) and velocity error $(\dot{e})$ asymptotically reach the origin while the parameter estimation error $(\tilde{\Theta}_2)$ remains bounded.

Proof: Consider a Lyapunov like function for the system defined as,

$$V = \frac{1}{2}\left(s^\top M_0 s + \tilde{\Theta}_2^\top \Gamma^{-1}\tilde{\Theta}_2\right) \geq 0$$

Differentiating V with respect to time and simplifying using the skew symmetry property and substituting the chosen adaptation law (8) we obtain,

$$\dot{V} = -s^\top D_0 s - s^\top K_s s \leq 0.$$

As $V \geq 0$ and $\dot{V} \leq 0$, $\lim_{t\to\infty} V$ is finite. Therefore, $s \in \mathcal{L}_2$ and $s, \tilde{\Theta} \in \mathcal{L}_\infty$. From (7), noting the properties of Lagrangian systems, we see that $\dot{s} \in \mathcal{L}_\infty$. Therefore, since $s \in \mathcal{L}_2$ and $\dot{s} \in \mathcal{L}_\infty$, we can show that $s \to 0$ as $t \to \infty$. Now from (4), $e, \dot{e} \to 0$ once $s = 0$. ■

B. Passivity-based robust control

Following the robust control approach in [10], and based off the adaptive control design, we use the control input as (6) with the parameter estimation vector $\hat{\Theta}_2$ now chosen as,

$$\hat{\Theta}_2 = \Theta_0 + u \quad (9)$$

where Θ_0 is a fixed nominal parameter vector and u is an additional control term which will be designed for achieving robustness for uncertain parameters. Hence, now we do not use any adaptation for the estimation of parameters. Using (9) in the control input (6) and substituting it in (2) yields,

$$M_0(q)\dot{s} + C_0(q, \dot{q})s + D_0 s + K_s s = Y_2(q, \dot{q}, v, a)(\tilde{\Theta}_0 + u) \quad (10)$$

where $\tilde{\Theta}_0 = \Theta_0 - \Theta_2$ is the parameter uncertainty which is constant. Suppose the uncertainty is bounded such that we can find a constant bound $\rho \geq 0$,

$$||\tilde{\Theta}_0|| = ||\Theta_0 - \Theta_2|| \leq \rho. \quad (11)$$

Then, letting $\epsilon > 0$, we can design the control term u as,

$$u = \begin{cases} -\rho\frac{Y_2^\top s}{||Y_2^\top s||} & \text{if} \quad ||Y_2^\top s|| > \epsilon \\ -\frac{\rho}{\epsilon}Y_2^\top s & \text{if} \quad ||Y_2^\top s|| \leq \epsilon \end{cases} \quad (12)$$

Theorem 2: Consider the closed loop system (10) with bounded parameter uncertainty as (11), the additional control u defined as (12) and the sliding surface (3). Then, the tracking error is uniformly ultimately bounded (u.u.b).

Proof: Consider a Lyapunov like function for the system defined as,

$$V = \frac{1}{2}s^\top M_0 s$$

Differentiating V with respect to time and simplifying yields,

$$\dot{V} = -s^\top Q s + s^\top Y_2(\tilde{\Theta}_0 + u)$$

where we have utilized the skew symmetric property and defined $Q := D_0 + K_s$. Considering the term $s^\top Y_2(\tilde{\Theta}_0 + u)$, we observe that if $||Y_2^\top s|| > \epsilon$ then,

$$\begin{aligned} s^\top Y_2(\tilde{\Theta}_0 + u) =& (Y_2^\top s)^\top \left(\tilde{\Theta}_0 - \rho \frac{Y_2^\top s}{||Y_2^\top s||} \right) \\ \leq& ||Y_2^\top s|| \left(||\tilde{\Theta}_0|| - \rho \right) < 0. \end{aligned}$$

which implies that $\dot{V} < 0$ with respect to s. Note that $||\tilde{\Theta}_0|| \leq \rho$ and $\rho \geq 0$. Hence, $\tilde{\Theta}_0 \leq \rho \frac{Y_2^\top s}{||Y_2^\top s||}$. Now, if $||Y_2^\top s|| \leq \epsilon$ then,

$$\begin{aligned} s^\top Y_2(\tilde{\Theta}_0 + u) =& (Y_2^\top s)^\top (\tilde{\Theta}_0 + u) \\ \leq& (Y_2^\top s)^\top \left(\rho \frac{Y_2^\top s}{||Y_2^\top s||} + u \right) \\ =& \rho ||Y_2^\top s|| - \frac{\rho}{\epsilon} ||Y_2^\top s||^2. \end{aligned}$$

The maximum of the R.H.S in the above expression is $\epsilon\rho/4$ which is achieved when $||Y_2^\top s|| = \epsilon/2$. Therefore,

$$\dot{V} \leq -s^\top Q s + \epsilon\rho/4$$

and see that $\dot{V} < 0$ if $s^\top Q s > \epsilon\rho/4$. Using the bounds on the quadratic form, $\lambda_{min}(Q)||s||^2 \leq s^\top Q s \leq \lambda_{max}(Q)||s||^2$, where, $\lambda_{min}(Q)$ and $\lambda_{max}(Q)$ are, respectively, the minimum and maximum eigenvlaues of the matrix Q, we have that $\dot{V} < 0$ if $\lambda_{min}(Q)||s||^2 > \epsilon\rho/4$ or, equivalently

$$||s|| > \left(\frac{\epsilon\rho}{4\lambda_{min}(Q)} \right) =: \delta.$$

The u.u.b follows from this result using δ to define the radius of the ultimate boundedness set. ■

IV. Subtask Control in Null Space

The HyRiSo robot is redundant, since the hybrid robot's degrees of freedom (α) is greater than the dimension of the task space (2). Thus, $null(J)$ has a minimum dimension of $(\alpha - 2)$ which can be exploited to accomplish a desired subtask control as the task space motion is not affected of the link velocity in the null space. This is done by designing the auxiliary function $\psi_s(t)$ in (3) appropriately [26]. In this work we design it in such a way that taking the negative gradient of a convex function $f(q)$ as,

$$\psi_s = -\frac{\partial}{\partial q} f(q), \tag{13}$$

whose minima leads to the desired state [25]. When there are multiple subtasks, the auxiliary function is the summation of the negative gradients.

We will consider the subtasks of achieving collision avoidance of the HyRiSo robot and accounting for joint limits in this note.

A. Collision avoidance

In this subtask, consider the location of an obstacle in the environment to be X_0. To avoid points X_{s_j}, $j \in \Omega$ on the HyRiSo robot (Ω is the set of points on the HyRiSo robot designed for collision avoidance) colliding with the obstacle, we define the convex function for the collision avoidance subtask as,

$$f^0_{\text{obs}_j}(q) = \left(\min \left\{ 0, \frac{d_{j0}^2 - R^2}{d_{j0}^2 - r^2} \right\} \right)^2$$

where $d_{j0} = ||X_{s_j} - X_0||$ is the distance between a point X_{s_j} on the robot and the obstacle X_0. Here R is the avoidance distance and r is the smallest safe distance of d_{j0}. The objective of this avoidance function is to guarantee that d_{j0} remains greater than the safe distance r by changing the configuration of the robot in the null space. The corresponding auxiliary function $(\psi^0_{s_j})$ for this subtask can be easily found using (13) [25].

In different applications there could be multiple points on the robot for collision avoidance (X_{s_j}, $j \in \Omega$) as well as multiple objects (X_k, $k = 1, 2, .., m$) in the environment. In that case, the auxiliary function for collision avoidance is the summation, $\psi_s = \sum_{k=1}^{m} \sum_{j \in \Omega} \psi^k_{s_j}$.

B. Joint angle limits

For the joint angle limit subtask we define the convex function,

$$f_{\text{joint}}(q) = \Pi_{j=1}^{\alpha} \left(\left(\frac{1}{q_j^{max} - q_j} \right) \left(\frac{1}{q_j - q_j^{min}} \right) \right)$$

where q_j is the joint angle of the j^{th} link with $j = 1, 2, ..., \alpha$. Here q_j^{max} and q_j^{min} denote the maximum and minimum allowable joint limits of the j^{th} link. The corresponding auxiliary function for this sub-task can be easily found using (13).

V. Numerical examples

A. The hybrid robot parameters

We employ a four DoF HyRiSo robot on the horizontal plane. The robot is composed of two rigid links and two soft links where the first two links are rigid and the last two links are soft. We considered the joints between R-S and S-S links to be fixed. The lengths of the manipulators are $L = [1, 1, 1, 1]^\top$m. The masses of the links are $m = [0.3, 0.3, 0.51, 0.51]^\top$kg. Ignoring the base motor as it does not contribute to the dynamics, the motor mass at the rigid-rigid joint is $m_m = 0.1$kg. The end effector mass is $m^* = 0.25$kg. The moment of inertia of the rigid links is given as $I = [0.025, 0.025]^\top \text{kg}\,\text{m}^2$. The stiffness of the two links $k = 0.03$ N/m, and the damping of the two links $d = 0.05$ Ns/m was assumed to be the same. The base of the robot is attached to the environment at the origin. Considering the actuator mapping, we assume that the two motor signals for the two revolute joints have the same scaling and the two bending signals for the two soft links have the same scaling, but different from that of the motor signals. Hence, we define $A = \text{diag}(a_1, a_1, a_2, a_2)$ with $a_1 = 2$ and $a_2 = 0.1$.

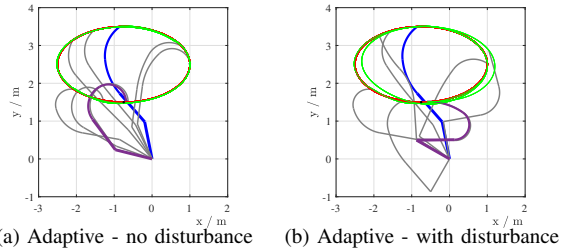

(a) Adaptive - no disturbance (b) Adaptive - with disturbance

(c) Robust - no disturbance (d) Robust - with disturbance

Fig. 2. Performance of the HyRiSo robot utilizing the designed controllers for trajectory tracking in an uncluttered environment with and without disturbance. The configuration plots illustrates the initial pose in blue, end pose in purple and intermediate poses in grey. The reference trajectory is plotted in red and the actual tip trajectory is overlaid in green.

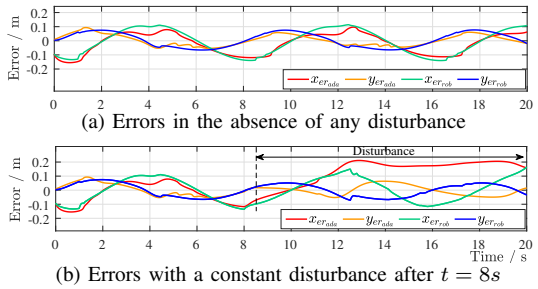

(a) Errors in the absence of any disturbance

(b) Errors with a constant disturbance after $t = 8s$

Fig. 3. Trajectory tracking errors for tracking an oblique circle.

The parameter vector was chosen as $\Theta_2 = [\frac{m_1}{a_1}, \frac{I_1}{a_1}, \frac{m_m}{a_1}, \frac{m_2}{a_1}, \frac{I_2}{a_1}, \frac{m_3}{a_1}, \frac{m_3}{a_2}, \frac{m_4}{a_1}, \frac{m_4}{a_2}, \frac{m^*}{a_1}, \frac{m^*}{a_2}, \frac{d}{a_2}, \frac{k}{a_2}]^\top$ with the nominal values chosen as $\hat{\Theta}_2(0) = 0.05\,\mathbf{1}^{13\times1} = \Theta_0$. Here $\mathbf{1}^{13\times1}$ is a 13×1 vector containing 1 as all entries. With this selection we can find the uncertainty bound $||\tilde{\Theta}_0|| \leq 7.576$, and we used $\rho = 8$ in our robust controller along with $\epsilon = 0.1$. For the adaptive controller we choose the adaptation gain $\Gamma = 2.75$ and the control gain $K_s = \mathbb{I}$ for all the scenarios. The tracking gain $\Lambda = 18\,\mathbb{I}_2$ was used in the adaptive controller, and $\Lambda = 12\,\mathbb{I}_2$ in the robust controller. The initial pose of the HyRiSo robot was $q(0) = [-\frac{\pi}{16}, -\frac{\pi}{6}, \frac{\pi}{5}, \frac{\pi}{3}]^\top$ with zero intial velocities for all the simulations.

B. Simulation results

We will discuss two scenarios - the first scenario is task space trajectory tracking of an oblique circle shape in an uncluttered environment and the second scenario is task space trajectory tracking of line segments in a cluttered environment. In both these scenarios we will test the adaptive controller and the robust controller under different conditions that will be discussed subsequently in the scenario descriptions.

1) Trajectory tracking of an oblique circle shape in uncluttered environment: In this scenario the reference trajectory $X_d(t) = [x_{ref}(t), y_{ref}(t)]^\top$ is defined as,

$$x_{ref}(t) = \quad -0.75 + 1.75\sin(0.25\pi t)$$
$$y_{ref}(t) = \quad 2.5 + \cos(0.25\pi t)$$

We considered two simulated experiments, one in which no external disturbance was involved and another with a constant disturbance of $F = [-2, 1]^\top N$ on the robot tip appearing at $t = 8s$ and remaining till the end of the simulation. The simulation results for these experiments are illustrated in Fig.2. The tracking errors are shown in Fig.3. We can observe that the two controllers have comparable performance in the experiment without any external disturbance. However, as soon as the external disturbance is introduced, the adaptive controller performs poorly while the robust controller performs similar to the experiment without any disturbances.

2) Trajectory tracking of line segments in a cluttered environment: In this scenario, the environment has two obstacles placed at $X_1 = [0.5,\ 1.5]^\top$ and $X_2 = [1.5,\ 1.5]^\top$. The smallest safe distance for both the obstacles was set to $r = 0.3m$ and the avoidance distance was set to $R = 0.7m$. We chose the base of the first and second soft links and the mid point of the second (last) soft link as the points on the robot to avoid obstacles. The reference trajectory in this scenario was defined as in Table I.

TABLE I

REFERENCE TRAJECTORY FOR COLLISION AVOIDANCE SCENARIO

Time / s	Reference trajectory ($X_d(t)$) / m
$0 \leq t < 2$	$[-0.75,\quad 3.25]^\top$
$2 \leq t < 5.75$	$[-0.75 + 0.2(t-2),\quad 3.25]^\top$
$5.75 \leq t < 17$	$[0,\quad 3.25 - 0.2(t-5.75)]^\top$
$17 \leq t < 27$	$[0.2(t-17),\quad 1]^\top$
$27 \leq t < 32$	$[2,\quad 1 + 0.2(t-27)]^\top$
$32 \leq t < 37$	$[2 - 0.2(t-32),\quad 2]^\top$
$37 \leq t \leq 39.5$	$[1,\quad 2 - 0.2(t-37)]^\top$
$39.5 \leq t$	$[1,\quad 1.5]^\top$

Fig.4 a,c illustrates the performance of the HyRiSo robot utilizing the designed controllers without activating the subtask control of collision avoidance. It is clearly seen that the robot collides with the obstacles in this case. However, we can assume that this simulation illustrates the trajectory tracking of line segments if the environment was uncluttered. Fig.4 b,d illustrates the efficacy of the subtask control which avoids any collisions with the obstacles while achieving trajectory tracking. This also showcases the dexterity of the HyRiSo robot. The tracking errors for these simulations are illustrated in Fig.5.

VI. Conclusion and Future Work

In this paper, we introduce a novel robotic system, a hybrid rigid-soft (HyRiSo) robot, that is composed of rigid links and soft links serially attached together. This class of robots are particularly interesting as they possess enhanced dexterity properties thanks to the additional soft links in the system. The hybrid nature of the robot introduces

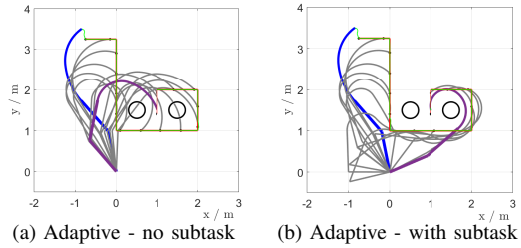

(a) Adaptive - no subtask (b) Adaptive - with subtask

(c) Robust - no subtask (d) Robust - with subtask

Fig. 4. Performance of the HyRiSo robot utilizing the passivity based controllers for trajectory tracking in the cluttered environment with and without the use of the sub-task for collision avoidance. The configuration plots on the top illustrates the initial pose in blue, end pose in purple and intermediate poses in grey. The reference trajectory is plotted in red and the actual tip trajectory is overlaid in green.

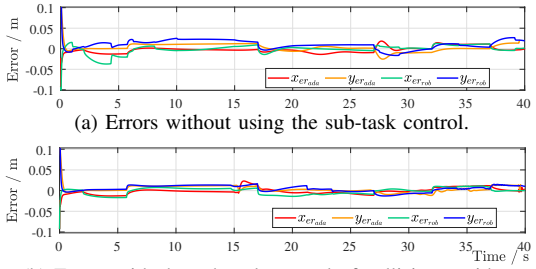

(a) Errors without using the sub-task control.

(b) Errors with the sub-task control of collision avoidance

Fig. 5. Trajectory tracking errors for the simulated experiments in the cluttered environment.

uncertainties in the parameters. An important note is that the heterogeneity in the mode of actuation for the revolute joints and the soft links. Hence, the uncertain actuator mapping plays an important role in controlling the class of hybrid robots. To that end, we designed two passivity-based controllers, an adaptive controller and a robust controller in this work to remedy this challenge. We illustrated the efficacy of the proposed hybrid robot with the designed controllers using numerical examples showcasing task space trajectory tracking in challenging workspaces. The future directions include validating the proposed controllers using a physical hybrid robot and extending this framework to the class of 3D spatial hybrid robots.

REFERENCES

[1] D. Rus and M. T. Tolley, "Design, fabrication and control of soft robots," *Nature*, vol. 521, no. 7553, pp. 467–475, 2015.

[2] C. Majidi, "Soft robotics: a perspective—current trends and prospects for the future," *Soft Robotics*, vol. 1, no. 1, pp. 5–11, 2014.

[3] S. Satheeshbabu, N. K. Uppalapati, G. Chowdhary, and G. Krishnan, "Open loop position control of soft continuum arm using deep reinforcement learning," in *2019 International Conference on Robotics and Automation (ICRA)*. IEEE, 2019, pp. 5133–5139.

[4] C. Laschi, B. Mazzolai, and M. Cianchetti, "Soft robotics: Technologies and systems pushing the boundaries of robot abilities," *Science Robotics*, vol. 1, no. 1, p. eaah3690, 2016.

[5] N. K. Uppalapati, B. Walt, A. Havens, A. Mahdian, G. Chowdhary, and G. Krishnan, "A berry picking robot with a hybrid soft-rigid arm: Design and task space control," *Proceedings of Robotics: Science and Systems, Corvalis, Oregon, USA*, p. 95, 2020.

[6] R. Ortega and M. W. Spong, "Adaptive motion control of rigid robots: A tutorial," *Automatica*, vol. 25, no. 6, pp. 877–888, 1989.

[7] J. . E. Slotine and L. Weiping, "Adaptive manipulator control: A case study," *IEEE Transactions on Automatic Control*, vol. 33, no. 11, pp. 995–1003, Nov 1988.

[8] J.-J. E. Slotine and W. Li, "Composite adaptive control of robot manipulators," *Automatica*, vol. 25, no. 4, pp. 509–519, 1989.

[9] H. Wang, "Adaptive control of robot manipulators with uncertain kinematics and dynamics," *IEEE Transactions on Automatic Control*, vol. 62, no. 2, pp. 948–954, 2016.

[10] M. Spong, "On the robust control of robot manipulators," *IEEE Transactions on Automatic Control*, vol. 37, no. 11, pp. 1782–1786, 1992.

[11] C. Abdallah, D. M. Dawson, P. Dorato, and M. Jamshidi, "Survey of robust control for rigid robots," *IEEE Control Systems Magazine*, vol. 11, no. 2, pp. 24–30, 1991.

[12] C.-C. Cheah, C. Liu, and J.-J. E. Slotine, "Adaptive jacobian tracking control of robots with uncertainties in kinematic, dynamic and actuator models," *IEEE transactions on automatic control*, vol. 51, no. 6, pp. 1024–1029, 2006.

[13] T. Rugthum and G. Tao, "Adaptive actuator failure compensation for cooperative robotic manipulators with parameter uncertainties," *International Journal of Adaptive Control and Signal Processing*, vol. 35, no. 9, pp. 1916–1940, 2021.

[14] A. Kazemipour, O. Fischer, Y. Toshimitsu, K. W. Wong, and R. K. Katzschmann, "Adaptive dynamic sliding mode control of soft continuum manipulators," *arXiv preprint arXiv:2109.11388*, 2021.

[15] L. Weerakoon and N. Chopra, "Bilateral teleoperation of soft robots under piecewise constant curvature hypothesis: An experimental investigation," in *2020 American Control Conference (ACC)*, 2020, pp. 2124–2129.

[16] M. Trumić, C. Della Santina, K. Jovanović, and A. Fagiolini, "Adaptive control of soft robots based on an enhanced 3d augmented rigid robot matching," in *2021 American Control Conference (ACC)*. IEEE, 2021, pp. 4991–4996.

[17] L. Weerakoon, Z. Ye, R. S. Bama, E. Smela, M. Yu, and N. Chopra, "Adaptive tracking control of soft robots using integrated sensing skins and recurrent neural networks," in *2021 IEEE International Conference on Robotics and Automation (ICRA)*. IEEE, 2021, pp. 12 170–12 176.

[18] F. Hisch, A. Giusti, and M. Althoff, "Robust control of continuum robots using interval arithmetic," *IFAC-PapersOnLine*, vol. 50, no. 1, pp. 5660–5665, 2017.

[19] I. Robert J. Webster and B. A. Jones, "Design and kinematic modeling of constant curvature continuum robots: A review," *The International Journal of Robotics Research*, vol. 29, no. 13, pp. 1661–1683, 2010.

[20] C. Della Santina, R. K. Katzschmann, A. Bicchi, and D. Rus, "Model-based dynamic feedback control of a planar soft robot: trajectory tracking and interaction with the environment," *The International Journal of Robotics Research*, vol. 39, no. 4, pp. 490–513, 2020.

[21] V. Falkenhahn, T. Mahl, A. Hildebrandt, R. Neumann, and O. Sawodny, "Dynamic modeling of constant curvature continuum robots using the euler-lagrange formalism," in *2014 IEEE/RSJ International Conference on Intelligent Robots and Systems*, 2014, pp. 2428–2433.

[22] M. W. Spong, S. Hutchinson, and M. Vidyasagar, *Robot modeling and control*. John Wiley & Sons, Inc., 2006.

[23] G. Tonietti and A. Bicchi, "Adaptive simultaneous position and stiffness control for a soft robot arm," *IEEE/RSJ International Conference on Intelligent Robots and Systems*, vol. 2, pp. 1992–1997 vol.2, 2002.

[24] M. Trumić, K. Jovanović, and A. Fagiolini, "Decoupled nonlinear adaptive control of position and stiffness for pneumatic soft robots," *The International Journal of Robotics Research*, vol. 40, no. 1, pp. 277–295, 2021.

[25] Y.-C. Liu and N. Chopra, "Control of semi-autonomous teleoperation system with time delays," *Automatica*, vol. 49, no. 6, pp. 1553–1565, 2013.

[26] P. Hsu, J. Mauser, and S. Sastry, "Dynamic control of redundant manipulators," *Journal of Robotic Systems*, vol. 6, no. 2, pp. 133–148, 1989.